Phase Separating Bulk Metallic Glass: A Hierarchical Composite

Byung Joo Park,[1] Hye Jung Chang,[1] Do Hyang Kim,[1] Won Tae Kim,[2] Kamanio Chattopadhyay,[3]
T. A. Abinandanan,[3] and Saswata Bhattacharyya[3]

[1]*Department of Metallurgical Engineering, Center for Noncrystalline Materials, Yonsei University, Seoul 120-749, Korea*
[2]*Division of Applied Science, Chongju University, Chongju 360-764, Korea*
[3]*Department of Metallurgy, Indian Institute of Science, Bangalore 560 012, India*
(Received 1 January 2006; published 22 June 2006)

Phase separating systems present a unique opportunity for designing composites with hierarchical microstructure at different length scales. We report here our success in synthesizing phase separating metallic glasses exhibiting the entire spectrum of microstructural possibilities expected from a phase separating system. In particular, we report novel core shell and hierarchical structures of spherical glassy droplets, resulting from critical wetting behavior and limited diffusion. We also report synthesis of a bulk phase separating glass in a metallic glass system. The combination of unique core shell and hierarchical structures in metallic glass systems opens a new avenue for the microstructure design of metallic glasses.

Because of the presence of a critical point, phase separating systems present a unique opportunity for designing composites with a hierarchical microstructure at different length scales and provide an opportunity for developing materials with unique properties [1–5]. Phase separating silicate glasses are well known and are widely studied for scientific understanding and technological exploitation [6–9]. Recently, considerable effort in developing new multicomponent metallic glassy alloys has been underway due to the emergence of bulk metallic glass as a potential engineering material [10–13]. However, early efforts to obtain phase separating metallic glass were mired in controversy [14–20]. This is primarily because the formation of metallic glass requires very high negative heat of mixing and thus runs contrary to the tenets of a phase separating system which needs repulsive interactions among atoms. It is only recently that a few limited evidences of the phase separating metallic glass appeared in the literature [21–23].

Development of a hierarchical microstructure in a glassy state is of potential interest in terms of shear band propagation (and potential strain hardening) as well as development of additional functional properties. There exists a series of glasses which contain aluminum and cobalt as critical alloying elements for glass formation [24,25]. They form glasses with early transition metals on rapid cooling. We have systematically explored this type of glasses and report here our success in synthesizing a range of quaternary phase separating glasses exhibiting the entire spectrum of microstructural possibilities expected from a phase separating system. In particular, we report a novel core shell structure of spherical glassy particles embedded in a glassy matrix due to the interplay between the critical wetting behavior of the phase separating system and the glass transition and novel hierarchical arrangements of glassy spheres. Finally, we shall present a first report of a bulk phase separating glass in this class of metallic glasses.

The results that will be presented concern two categories of glasses. First, we shall present results on glasses which contain a fixed amount of aluminum and cobalt (24 and 20 at. %, respectively). The rest is made up of yttrium and titanium of varying compositions from 20 to 60 at. %. In this case, the alloys are processed from its melt by the rapid solidification technique of melt spinning with a typical cooling rate of 10^6 K/s. In the second category, we present results of a successful synthesis of a bulk phase separating glass with an equal amount of zirconium and yttrium in addition to cobalt and aluminum ($Zr_{28}Y_{28}Al_{22}Co_{22}$). The latter is processed by injection casting in the form of 1, 2, and 3 mm rods.

The microstructural studies using a transmission electron microscope reveal strikingly unique arrangements of glassy droplets of differing contrast. Figures 1(a) and 1(c) show the transmission electron micrographs from two glasses having compositions $Ti_{45}Y_{11}Al_{24}Co_{20}$ and $Ti_{28}Y_{28}Al_{24}Co_{20}$, respectively. One can clearly observe the core shell structure of the spherical glassy phase (lighter contrast) embedded in a matrix of darker contrast [Fig. 1(a)]. Even though Y has a higher atomic number than Ti, the average electron density in a Y rich amorphous phase (light) is smaller than that in a Ti rich phase (dark) due to the large difference in atomic size between Y and Ti. The electron and x-ray diffraction patterns in the inset confirm their glassy structures. The matrix shows evidence of fine scale decomposition. Composition analysis using an energy dispersive spectrometer attached to the scanning transmission electron microscope indicates an average composition of $Y_{44.5}Ti_{8.8}Al_{36.9}Co_{9.8}$ for the light contrast phase. The matrix, on the other hand, is rich in Ti, having a composition of $Ti_{47.2}Y_{2.1}Al_{19.9}Co_{30.8}$. Although cobalt has a similar affinity with yttrium and titanium (the heat of mixing of cobalt in yttrium and titanium is -22 and -28 kJ/mole of an atom, respectively), it has primarily partitioned into the matrix. Similarly, the concentration of
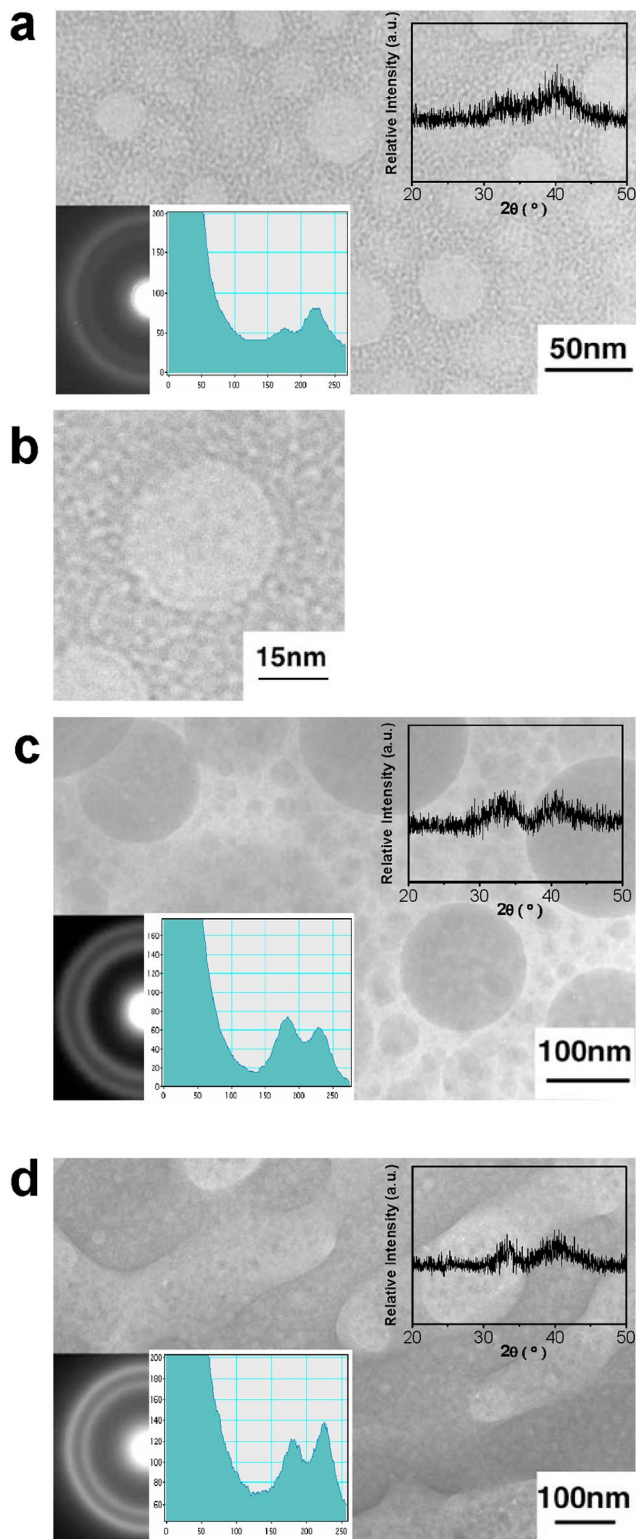
FIG. 1 (color online). Bright field transmission electron micrographs obtained from as-melt-spun (a) $Ti_{45}Y_{11}Al_{24}Co_{20}$, (c) $Ti_{28}Y_{28}Al_{24}Co_{20}$, (d) $Ti_{36}Y_{20}Al_{24}Co_{20}$, and alloys. (b) shows an enlarged view of one of the droplets shown in (a) to highlight the unique core shell structure of the droplets. The corresponding selected area diffraction patterns and digitized intensity profile are included in (a), (c), and (d).

aluminum is more in the droplet than in the matrix. An enlarged view of one of the droplets is shown in Fig. 1(b) to highlight the unique core shell structure of these droplets. In contrast, Fig. 1(c) shows droplets having a darker contrast embedded in the lighter matrix. The hierarchical structure of droplets of reversed contrast in the bigger droplets gives them a unique appearance. The finer droplets have a size of ~ 10 nm, while the larger droplets have an average size of ~ 220 nm. The overall composition of the larger droplets is $Ti_{49.7}Y_{3.8}Al_{14.7}Co_{31.8}$, while the matrix has a composition of $Y_{42.2}Ti_{7.3}Al_{35.1}Co_{15.4}$.

The microstructure of the alloys in between these two compositions shows a typical coarsened spinodal structure of two interpenetrating glassy phases. Figure 1(d) shows an example of this. The evidence of a droplet structure of reversed contrast is present within both the phases. The phases are still in a glassy state as evidenced from the electron diffraction pattern shown in the inset with two clear strong diffuse peaks. The composition analysis of the two phases give a yttrium rich composition of $Y_{38.8}Ti_{12.8}Al_{37.1}Co_{11.3}$ for the light phase while a titanium rich composition of $Ti_{43.3}Y_{3.7}Al_{15.3}Co_{37.7}$ for the darker phase.

We shall now attempt to explain the above results in terms of competition between the kinetics of phase separation and the approach to glass transition due to the kinetics of heat transfer. First, we show that, in spite of a strong glass former, the system indeed has a miscibility gap reflecting the strong repulsive interaction between yttrium and titanium. The binary phase diagram of these two elements exhibits a miscibility gap with a low dome height (expressed as the difference between the monotectic horizontal and the critical point, 172 K in the present case). Using a subregular solution model [26], the free energy of the liquid can be obtained from the expression

$$G = RT\sum_i x_i \ln x_i + \sum_{i=1}^{n} \sum_{j=i+1}^{n} x_i x_j \sum_{\nu=0} \Omega^{\nu} ij (x^i - x^j)^{\nu},$$

where Ω_{ij} represents the interaction parameter between the i and j components. The free energy curves of a Ti-Y-Al-Co system at a temperature range of 400–1200 K are calculated for a constant aluminum and cobalt composition of 24 and 20 at. %, respectively. The calculated free energy curves at a lower temperature range exhibit dome bounding regions of immiscibility, while those at a higher temperature range exhibit a single minimum. The pseudobinary phase diagram of the liquid phases based on the calculated free energy curves is shown in Fig. 2. The diagram also includes the spinodal boundaries where the second derivative of the free energy function goes to zero. Note that the pseudobinary section is shown here only to illustrate the situation. The tie line for any composition within the miscibility gap may or may not lie in this plane.

Let us consider the origin of the core shell structure of the droplets shown in Figs. 1(a) and 1(b). In Fig. 2, we have
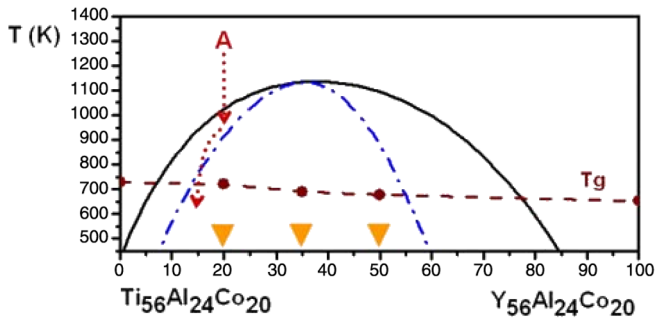
FIG. 2 (color online). Pseudobinary phase diagram of the liquid phases in a Ti-Y-Al-Co system calculated using a subregular solution model at a temperature range of 400–1200 K for a constant aluminum and cobalt composition of 24 and 20 at. %, respectively. The diagram includes the spinodal boundary (dashed-dotted line) and the glass transition temperature (T_g) (dotted line).

also included the experimentally observed upper glass transition temperatures obtained through differential scanning calorimetry of the melt spun alloys. Crossing this temperature will dramatically slow down the kinetics of phase decomposition due to a large increase in viscosity and, hence, a concomitant decrease in diffusivity. This will effectively quench the structure evolved at this point. Under the condition of a high cooling rate, the alloy "A" will first nucleate a liquid rich in yttrium as it enters the miscibility gap. However, the decomposition will not go to completion due to the reduced time available for mass transport due to the high cooling rate, and the matrix will follow a path similar to that shown schematically by the dotted line in Fig. 2. In case the matrix composition reaches the spinodal above the glass transition temperature (T_g), a spinodal phase separation will occur. Cahn [27] has shown that in such a situation the presence of any other interface will lead to what is termed as "critical wetting" at temperatures between the critical temperature (T_c) and a wetting transition temperature (T_w). One of the evolving phases of the spinodal decomposition will wet the interface and form an intruding layer between the decomposing matrix and the third phase. In most of the organic liquids, this happens at temperatures very close to the critical temperature. However, for metallic alloys, the wetting can occur at temperatures substantially lower than the critical point [28–30]. In order to predict the nature of the microstructure that evolves in such a situation, we have carried out a phase filed modeling of the microstructure that will evolve in the presence of a prenucleated liquid in a matrix which is decomposing spinodally. The model assumes isotropic properties applicable for phase separating glasses. These clearly show the evolution of a core shell-like structure due to critical wetting. The evolved microstructure with the wetted layer around the primary nucleated phase in the liquid with the composition corresponding to the left side of the critical point is shown in

Fig. 3, which is consistent with the experimental observation. For the case in Fig. 1(c), the change in liquid composition is not adequate for the liquid to enter the spinodal regime, as there is a wider separation between the spinodal boundary and the binodal line near this composition and the phase separation can occur only by nucleation and growth. However, due to the high cooling rates, the time available for the matrix and the separating droplets to equilibrate is insufficient and, hence, on further cooling, will lead to supersaturation of both decomposing phases. In such a situation, a driving force will develop for secondary nucleation inside these two phases, leading to the formation of droplets rich in yttrium and titanium, respectively, at a nanometric scale yielding a hierarchical structure. In the case of alloy melts entering the spinodal regime, the liquid decomposes spontaneously inside the spinodal domain with the composition fluctuation growing due to uphill diffusion [31]. However, once the composition reaches the spinodal boundary, the spontaneous decomposition ceases. The driving force for further decomposition at this stage is available which leads to a nucleation and growth process as the composition moves between the spinodal and binodal boundaries.

In a glass forming system, the viscosity of the melt and hence diffusivities of the species change significantly with the reduction in temperature during the cooling process. Therefore, following spinodal decomposition, a secondary decomposition within the spinodally decomposed regions (where the compositions will now be between the binodal and spinodal boundaries) by nucleation will set in, characterized by a smaller length scale. This is shown in Fig. 1(d), which again provides the opportunity of designing a hierarchical microstructure.

Following the success in synthesizing a phase separating metallic glass, we have explored the possibility of synthesizing a phase separating bulk metallic glass and succeeded in obtaining one in a Zr-Y-Al-Co system. To the best of our knowledge, such a report of phase separating bulk metallic glass is not available in the current literature. Figure 4
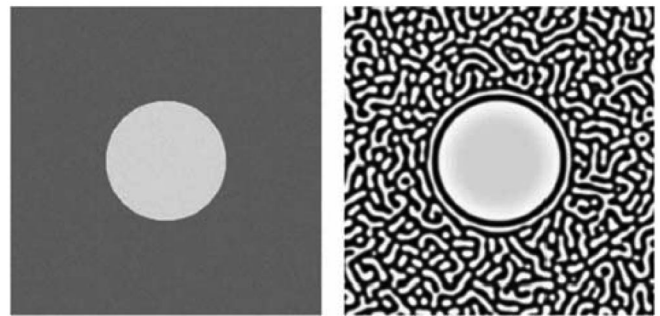

FIG. 3. Phase field modeling showing the evolution of a microstructure with the wetted layer around the primary nucleated phase in the liquid with the composition corresponding to the left side of the critical point.
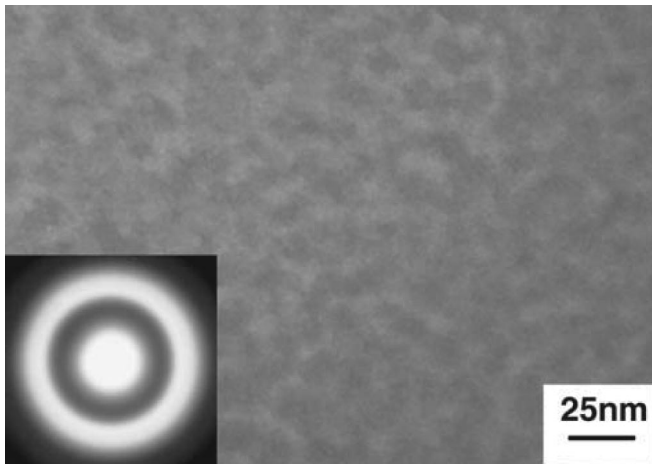
FIG. 4. Bright field transmission electron micrographs obtained from an as-injection-cast $Zr_{28}Y_{28}Al_{22}Co_{22}$ alloy (diameter: 3 mm). The corresponding selected area diffraction pattern is included in the figure.

shows the microstructure of the bulk glass of composition $Zr_{28}Y_{28}Al_{22}Co_{22}$. The morphology suggests that the decomposition has most likely taken place in the spinodal regime. This microstructure is obtained from a sample obtained from a 3 mm diameter cast rod. The inset shows the electron diffraction pattern exhibiting the superimposed halos from the phase separated zirconium rich and yttrium rich glasses. The scale of decomposition is finer for the 1 and 2 mm diameter cast rods, suggesting a glass transition has intervened the decomposition process earlier due to the higher cooling rates in these cases. Because of the lack of data for the interaction parameter between Zr and Co, we could not compute the critical point of this glass. But the experimental results suggest that the glass transition temperature is close to the critical point of this glass. Thus, we are unable to get nucleation controlled morphologies of the glassy sphere.

In conclusion, we confirm the possibility of phase separation of both melt spun and bulk metallic glass. We show that the interaction of critical point wetting and rapid solidification can lead to a unique core shell structure and a hierarchical microstructure which opens a new avenue for the microstructure design involving metallic glass.

[1] J. D. Mackenzie, J. Non-Cryst. Solids **26**, 458 (1977).
[2] W. Haller, Nature (London) **206**, 693 (1965).
[3] H. H. Weetall, Biochim. Biophys. Acta **212**, 1 (1970).
[4] A. R. Cooper and F. F. Johnson, J. Appl. Polym. Sci. **13**, 1487 (1969).
[5] I. S. Patel, P. W. Schmidt, and S. M. Ohlberg, J. Appl. Phys. **43**, 1636 (1972).
[6] J. Zarzycki, Discuss. Faraday Soc. **50**, 122 (1970).
[7] J. S. Langer, Ann. Phys. (N.Y.) **65**, 53 (1971).
[8] P. F. James, J. Mater. Sci. **10**, 1802 (1975).
[9] D. R. Uhlmann and A. G. Kolbeck, Phys. Chem. Glasses **17**, 146 (1976).
[10] W. L. Johnson, MRS Bull. **24**, 42 (1999).
[11] A. Inoue, Acta Mater. **48**, 279 (2000).
[12] Jörg F. Löffler, Intermetallics **11**, 529 (2003).
[13] W. H. Wang, C. Dong, and C. H. Shek, Mater. Sci. Eng., R **44**, 45 (2004).
[14] L. E. Tanner and R. Ray, Scr. Metall. **14**, 657 (1980).
[15] D. Nagahama, T. Ohkubo, and K. Hono, Scr. Mater. **49**, 729 (2003).
[16] R. Busch, S. Schneider, A. Peker, and W. L. Johnson, Appl. Phys. Lett. **67**, 1544 (1995).
[17] S. Schneider, P. Thiyagarajan, and W. L. Johnson, Appl. Phys. Lett. **68**, 493 (1996).
[18] W. H. Wang, Q. Wei, and S. Friedrich, Phys. Rev. B **57**, 8211 (1998).
[19] B. Van de Moortèle, T. Epicier, J. M. Pelletier, and J. L. Soubeyroux, J. Non-Cryst. Solids **345–346**, 169 (2004).
[20] I. Martin, T. Ohkubo, M. Ohnuma, B. Deconihout, and K. Hono, Acta Mater. **52**, 4427 (2004).
[21] B. J. Park, H. J. Chang, W. T. Kim, and D. H. Kim, Appl. Phys. Lett. **85**, 6353 (2004).
[22] A. A. Kündig, M. Ohnuma, H. H. Ping, T. Ohkubo, and K. Hono, Acta Mater. **52**, 2441 (2004).
[23] N. Mattern, U. Kühn, A. Gebert, T. Gemming, M. Zinkevich, H. Wendrock, and L. Schultz, Scr. Mater. **53**, 271 (2005).
[24] F. Guo and S. J. Poon, Appl. Phys. Lett. **83**, 2575 (2003).
[25] T. Wada, T. Zhang, and A. Inoue, Mater. Trans., JIM **43**, 2843 (2002).
[26] J. B. Thompson, *Thermodynamic Properties of Simple Solutions* (Wiley, New York, 1967) Vol. 2, p. 340.
[27] J. W. Cahn, J. Chem. Phys. **66**, 3667 (1977).
[28] H. Tostmann, E. DiMasi, O. G. Shpyrko, P. S. Pershan, B. M. Ocko, and M. Deutsch, Phys. Rev. Lett. **84**, 4385 (2000).
[29] D. Chatain and P. Wynblatt, Surf. Sci. **345**, 85 (1996).
[30] D. Nattland, P. D. Poh, S. C. Muller, and W. Freyland, J. Phys. Condens. Matter **7**, L457 (1995).
[31] J. W. Cahn, Trans. Metall. Soc. AIME **242**, 166 (1968).